Polyvinyl pyrrolidone-modified Pd/Fe nanoparticles for enhanced dechlorination of 2,4-dichlorophenal

Xiangyu Wang*, Fang Li, Jiacheng Yang

Faculty of Environmental Science and Engineering, Kunming University of Science and Technology, Kunming 650500, China
Tel. +86 0871 65189366; email: famdct@sohu.com

ABSTRACT

Dechlorination of chlorinated organic compounds with zero-valent iron or iron-based bimetallic nanoparticles (NPs) is an innovative technology for environmental remediation in soil and groundwater. However, dechlorination efficiency can be dramatically decreased due to aggregation of NPs. In this study, Pd/Fe NPs were modified by coating with polyvinyl pyrrolidone (K30) (PVP-K30) and PVP/ethanol as dispersants, respectively, resulting in not only the prevention of particle aggregation, but also the enhancement of overall dechlorination effectiveness. Transmission electron microscope, scanning electron microscope, specific surface area, and X-ray diffraction analyses indicate the dispersant-modified Pd/Fe NPs with a diameter of 50–100 nm were α-bcc crystal structure, highly dispersed with particle size distribution relatively uniform, and the majority of NPs are spherical particles. In comparison, the batch dechlorination tests demonstrated that the dispersant-modified Pd/Fe NPs exhibited higher dechlorination rate than pristine Pd/Fe NPs under same reaction condition. Additionally, some important parameters of catalytic dechlorination of 2,4-DCP with modified Pd/Fe NPs, such as pH value, temperature, and dosage of Pd/Fe NPs were also optimized.

Keywords: PVP; Modification; Pd/Fe nanoparticles; Dechlorination

1. Introduction

2,4-dichlorophenol (2,4-DCP) is an ubiquitous chlorinated aromatic organic compound in both wastewater and fresh water, which has aroused considerable scientific interests in its detoxification due to noteworthy toxicity and recalcitrant nature in the environment [1]. 2,4-DCP is extensively applied in industry and agriculture as wood preservers, pesticides, herbicides, biocides, dyes, etc. According to the

recommendation of the World Health Organization, the maximum concentration level for 2,4-DCP in drinking water is 70 ppb [2,3]. Generally, physical, chemical, and biological methods (such as activated carbon adsorption, incineration, catalytic oxidation, and biodegradation) have been applied for removal of chlorinated organic compounds. Even though biological treatment is superior due to its little possibilities of causing a secondary pollution, the poor biodegradability of 2,4-DCP and the byproducts might result in the inhabitation of their bioremediation. The catalytic reductive dechlorination of chlorinated aromatic

*Corresponding author.

compounds in aqueous solution by using Pd/Fe bimetallic nanoparticles (NPs), in which Fe acts as reductant and Pd acts as hydrocatalyst, provides an effective approach for removal of 2,4-DCP [4,5]. Nanoscale Pd/Fe bimetallic particles are found to be superior to mono-Fe0 reductant and other iron-based bimetals (e.g. Ni/Fe, Cu/Fe, and Pt/Fe) for dechlorination of 2,4-DCP because of the large surface area and high hydrogenation activity of Pd [6–10]. Lately, zero-valent iron (ZVI) or iron-based bimetal technologies are applied for *in situ* dechlorination by direct injection of NPs into contaminated water and groundwater. This cost-effective and timesaving *in situ* technology has already attracted increasing interest. Large specific surface area of Fe NPs provides more active sites for the degradation of contaminants resulting in the high reactivity for dechlorination. However, NPs tend to agglomerate easily to micro scale or even larger scale powders in aqueous solution [11]. The aforementioned drawback could cause the decrease of their catalytic dechlorination activity, and it is considered one of the biggest technical barriers for the wide application of ZVI technology. In recent studies, the following two approaches were used for dispersion of NPs: (1) immobilizing NPs on surface of solid supports as stabilizer, such as activated bentonite [12], alumina [13], and silicon oxides [14,15]; (2) coating NPs with dispersants to prevent the agglomeration between particles through the electrostatic repulsion and/or steric hindrance between the dispersant-coated NPs [16–18]. The latter method is superior to the former because the mass transfer is lowered to a large extent due to the dense structure of the solid supports by using solid immobilization method. Consequently, the enhanced catalytic activity dispersant-coated Pd/Fe NPs would be inevitably affected by the synthesis conditions.

In previous studies, an effective method for increasing colloidal stability, mobility, and reactivity in the subsurface of NPs is the surface modification by surfactants [19] and polyelectrolyte coatings [20–23]. But, most modifiers are environmentally harmful, such as cetyl trimethyl amnium bromide [19], and they can easily cause secondary pollution to the environment. However, some polymers are environmentally friendly, such as soluble starch [24,25] and guar gum [26]. This research is aimed to provide an effective modification method for preparation of polymer functionalized Pd/Fe NPs to enhance the catalytic dechlorination activity for removal of chlorinated organic compounds. Polyvinyl pyrrolidone (PVP) was used as a dispersing agent to functionalize Pd/Fe NPs, while 2,4-DCP was chosen as target pollutant. Its role

is twofold: (1) acting as a stabilizing agent, preventing aggregation of metal particles, and (2) retaining a uniform colloidal dispersion. Additionally, PVP is used as a shape-controlling agent or "a crystal-habit modifier", promoting attachment of metal atoms onto the specific crystal faces and leading to the highly anisotropic growth of nuclei into nanostructure. Containing a hydroxyl, anhydrous ethanol plays a catalytic role in the dispersion of NPs. In order to improve the dispersity of Pd/Fe NPs and the dechlorination efficiency of 2,4-DCP by PVP functionalized Pd/Fe NPs, anhydrous ethanol was added into reaction solution during preparation process of PVP functionalized Pd/Fe NPs. The effects of different modification methods on dechlorination activity of PVP modified Pd/Fe NPs were evaluated. In addition, mechanisms of the removal of 2,4-DCP from water by Pd/Fe NPs with or without PVP functionalization were elucidated according to the dechlorination kinetics.

2. Experimental

2.1. Materials

Ferrous sulfate heptahydrate (FeSO$_4$·7H$_2$O, CAS No. 7782-63-0), potassium borohydride (KBH$_4$, CAS No. 13762-51-1), ethanol (C$_2$H$_6$O, CAS No. 64-17-5), acetone (C$_3$H$_6$O, CSA No. 67-64-1), and PVP ((C$_6$H$_9$NO)$_n$, CSA No. 9003-39-8) were obtained from Kermel (Tianjin, China); 2,4-dichlorophenol (2,4-DCP, CAS No. 120-83-2), p-chlorophenol (4-CP, CAS No. 106-48-9), o-chlorophenol (2-CP, CAS No. 95-57-8), and phenol (P, CAS No. 108-95-2) were obtained from Ourchem (Sinopharm Chemical Reagent Co. Ltd.). Palladium acetate ([Pd(C$_2$H$_3$O$_2$)$_2$]$_3$, CAS No. 3375-31-3), from Aldrich. All chemicals were analytic reagents, and were used as received.

2.2. Preparation and characterization of dispersant-coated Pd/Fe NPs

Preparation of NPs was carried out in an anaerobic chamber, into which nitrogen gas was continuously flowed in an effort to prevent the oxidation of freshly prepared NPs. Dispersant-coated Fe NPs were prepared by adding 250 mL of 0.2 mol/L KBH$_4$ solution dropwise to 200 mL of 1.0 mol/L FeSO$_4$ solution containing desired concentration of dispersant under vigorous magnetic stirring for complete mixing. Fe NPs were prepared according the following equation:

$$Fe^{2+} + BH_4^- + H_2O \rightarrow Fe^0 \downarrow + H_2BO_3^- + 2H^+ + H_2 \uparrow \quad (1)$$
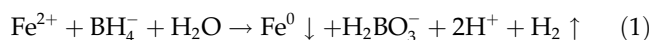
Before the preparation of modified Pd/Fe NPs, PVP was added as a dispersant into $FeSO_4$ solution, and the concentrations differed from 0.2 wt% to 5.0 wt% (mass rate). The solvent of $FeSO_4$ solution was a mixed solution of deionized water and ethanol, and ethanol adding ratio was 1:9–1:3 (volume ratio). All solutions were stirred vigorously before being used for preparation of iron NPs.

And next, Fe NPs were charged into ethanol solution of palladium acetate under magnetic stirring for 30 min, resulting in the reduction of Pd^{2+} and deposition of Pd on Fe NPs surface:

$$Pd^{2+} + Fe \rightarrow Pd + Fe^{2+} \tag{2}$$

2.3. Batch 2,4-DCP dechlorination experiments

For each dechlorination reaction (Eq. (3)), 100 ml deionized water was filled into 250 ml volume serum bottles. 2,4-DCP solution with an initial concentration of 20 mg/L was loaded with certain amount of PVP-modified Pd/Fe NPs, and sealed immediately with Teflon-lined rubber septums. These bottles were agitated at a constant shaking rate of 170 rpm in a temperature-controlled orbital shaker. Parallel experiments were conducted with the same amount of pristine Pd/Fe NPs under the similar reaction conditions. At each sampling time, aliquots of samples were taken from the supernatant with a hermetic syringe. After being filtered through strainer installs a 0.22-μm microfiltration membrane, the solution in the syringe was used for subsequent analyses. Triplicate experiments were performed to get the average values.

$$Fe + RCl_n + H \xrightarrow{Pd} Fe^{2+} + RCl_{n-1}H + Cl^- \tag{3}$$

2.4. Characterization of Pd/Fe NPs

Morphological structures of pristine Pd/Fe NPs and modified Pd/Fe NPs were characterized by using a scanning electron microscope (SEM). Firstly, immobilized Pd/Fe NPs were put onto the surface of conducting resin, followed by blowing off the Pd/Fe NPs that floated on the surface, and metal gold were sprayed onto NPs to enhance electric conductivity. Then, images of samples were observed by the SEM.

The specific surface areas of dispersant-coated Pd/Fe NPs were measured from N_2 physisorption using Barrett–Joyner–Halenda and multipoint BET (Brunauer–Emmett–Teller) methods with a TriStar II

3020 V1.03 analyzer (Micromeritics Instrument Corporation).

The particle size and dispersion conditions of modified and unmodified Pd/Fe NPs were observed with JEM 1200EX transmission electron microscope (TEM, JEOL Ltd., Japan) at an acceleration voltage of 120 kV. Before being visualized under TEM lens, Pd/Fe NPs were ultrasonic in acetone for 5 min, and the suspended solution was dropped and air-dried on a 300-mesh gold/copper lacey carbon grid.

The crystal structures of modified and unmodified Pd/Fe NPs were characterized by X-ray diffraction (XRD) on a D/max-rB X-ray diffractometer (Rigaku Corp., Japan) using Ni-filtered Cu Kα radiation operating at an accelerating voltage of 45 kV, emission current of 40 mA, and λ of 0.15418 nm in a step scanning mode, with a step size of 0.02° and a counting time of 1 s per step in the range 20–90°. The crystal diameters of Pd/Fe NPs were calculated by Scherrer diffraction formula.

2.5. Analytical method

The concentrations of the parent-chlorinated organic compounds and byproducts or/and final product were measured with a 1260 HPLC (Agilent). A mixture of methanol and water (methanol: deionized water = 6:4 (v/v)) was used as an eluent with a flow rate of 1.0 mL/min at a wavelength of 283 nm. The size of sample loop was 10 μl. The wavelength of the detector was set at 280 nm. Calibration of HPLC was conducted prior to each set of measurements, and the final result is the average of the triplicate estimated values.

3. Results and discussion

3.1. Characterization of Pd/Fe bimetallic NPs

SEM images for pristine Pd/Fe NPs and PVP-modified Pd/Fe NPs are shown in Fig. 1(a)–(c). It is obvious that pristine Pd/Fe NPs agglomerated severely, and the appearance of NPs is indistinct. From Fig. 1(b) and (c), the dispersities of PVP-modified Pd/Fe NPs (PVP-Pd/Fe) and PVP/ethanol-modified NPs (PVP/ethanol-Pd/Fe NPs) were improved distinctly and the outlines of two kinds of Pd/Fe NPs are comparative clear. That is mainly due to the dispersing capability of PVP and ethanol to Pd/Fe NPs. PVP is a linear polymer that is widely used as a protecting agent in the synthesis of monodisperse metal and semiconductor NPs. With the pyrrolidone functional groups, this polymer cap is expected to
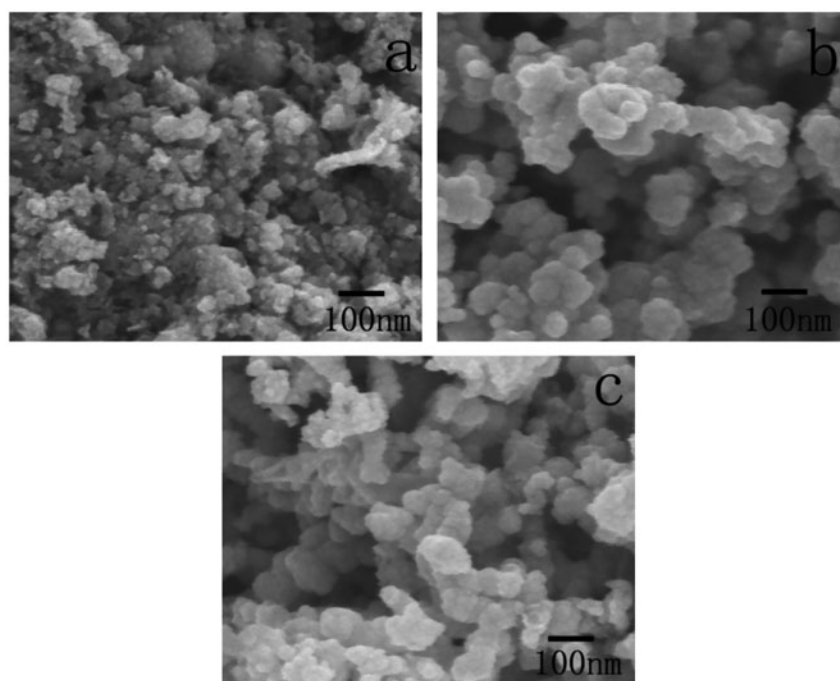
Fig. 1. SEM images of Pd/Fe NPs: (a) pristine Pd/Fe NPs, (b) PVP-Pd/Fe NPs (ethanol adding ratio is 0), (c) PVP-Pd/Fe NPs (ethanol adding ratio is 1:3).

arrest the nascent Fe NPs efficiently, resulting in a narrow size distribution of modified NPs. With a hydroxyl group, the presence of ethanol can also promote the dispersibility of Pd/Fe NPs. The BET-measured specific area (SBET) of synthesized pristine Pd/Fe, PVP-Pd/Fe, and PVP/ethanol-Pd/Fe NPs are 26.8, 23.3, and $25.4\,m^2\,g^{-1}$, respectively. As can be seen, with the addition of PVP or PVP/ethanol, the surface areas of Pd/Fe NPs were effectively reduced. Therefore, aggregation of Pd/Fe NPs could be reduced with the addition of PVP dispersant, which could provide the necessary repulsive force to block the magnetic attraction among zero-value iron NPs. Although, with the coating of PVP dispersant, the particle diameters of modified Pd/Fe NPs were slightly increased, resulting in the decrease of the BET-measured specific surface area; the coating of PVP is beneficial to the dispersion of NPs and could greatly enhance the reactivity of the particles in dechlorination of 2,4-DCP.

The XRD patterns of pristine and PVP-modified Pd/Fe NPs before dechlorination 2,4-DCP are shown in Fig. 2. From Fig. 2(a), four diffraction peaks for Fe(0) (2 theta = 35.62, 44.80, 64.78, and 82.63°) were observed in the XRD pattern of pristine Pd/Fe NPs, while three diffraction peaks were found (2 theta = 44.80, 64.78, and 82.63°) for modified Pd/Fe NPs. Comparing with the standard powder diffraction file cards of ZVI, iron oxi-
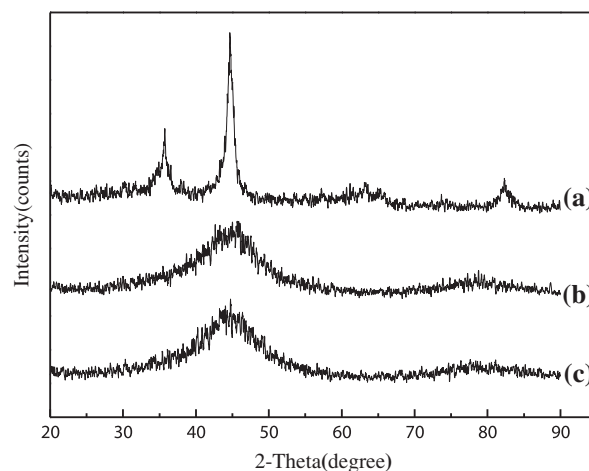
Fig. 2. XRD patterns of Pd/Fe NPs: (a) pristine Pd/Fe NPs, (b) PVP-Pd/Fe NPs (ethanol adding ratio is 0), (c) PVP-Pd/Fe NPs (ethanol adding ratio is 1:3).

des can be found in pristine Pd/Fe NPs (2 theta = 35.62°). This indicates that unmodified Pd/Fe NPs were oxidized, and this result is consistent with the SEM images. But no characteristic peaks of iron oxides can be found in Fig. 2(a) and (b). The reason might be that PVP coated on the surface of Pd/Fe NPs acted as a protective layer, it could not only prevent the particles from agglomeration, but also the exposure of particles to air. Observed from Fig. 2, the peaks of modified

Pd/Fe NPs are weaker than that of pristine one. This is consistent with the results reported by Guo et al. and Chen et al. [27,28].

Fig. 3 exhibits the TEM images of the pristine, PVP-Pd/Fe NPs, and PVP/ethanol-Pd/Fe NPs. Fig. 3 (a) shows the blurred appearance of Pd/Fe NPs, which indicate the severe agglomeration. From Fig. 3 (b) and (c), modified Pd/Fe NPs could be easily distinguished from each others. And the diameters of PVP-modified Pd/Fe NPs are in the range of 50–100 nm. This implied that PVP-Pd/Fe and PVP/ethanol-Pd/Fe NPs had higher dispersity than pristine ones. These results shown in TEM images are in good agreement with that shown in SEM images. Notably, compared with pristine Pd/Fe NPs, the aggregation and conglomeration of PVP-Pd/Fe NPs and PVP/ethanol-Pd/Fe NPs can be significantly reduced, resulting in the increase of the stability of PVP-Pd/Fe NPs and PVP/ethanol-Pd/Fe NPs.

3.2. Optimum conditions for synthesis of PVP-modified Pd/Fe NPs

3.2.1. Effect of dispersant concentration on catalytic dechlorination activity of modified Pd/Fe NPs

Dechlorination efficiency of 2,4-DCP with PVP-modified Pd/Fe NPs under different additions is shown in Fig. 4. Compared with pristine NPs, the dechlorination efficiency of four kinds of PVP-modified Pd/Fe NPs with different amount of PVP addition was increased by 8%∼15%. While the addition amount of the dispersing reagent was within the range of 0.2–0.5 wt%, the dechlorination efficiency of 2,4-DCP was increased with increasing concentration of PVP. The reason might be that the dispersity and reactivity of PVP-Pd/Fe NPs could be enhanced with the increase of concentration of PVP. Throughout the duration of the dechlorination experiment, it could be seen that the optimal PVP addition in PVP-Pd/Fe NPs is 0.5 wt%. When the dispersant concentration is larger than the optimal concentration, the surface of Pd/Fe NPs would be totally coated with PVP; therefore, the chances of effective contact between target pollutants and Pd/Fe NPs during the dechlorination reaction were decreased, resulting in decrease of dechlorination efficiency. In addition, much more foam was formed in the preparation process of Pd/Fe NPs and the output of Fe NPs were inevitably reduced. The concentration of PVP was recommended 0.5 wt% in subsequent experiment.

3.2.2. Effect of ethanol addition ratio on catalytic dechlorination activity of PVP-Pd/Fe NPs

Effects of ethanol addition ratio on dechlorination efficiency of 2,4-DCP with PVP/ethanol-modified Pd/Fe NPs are shown in Fig. 5. As can be seen from
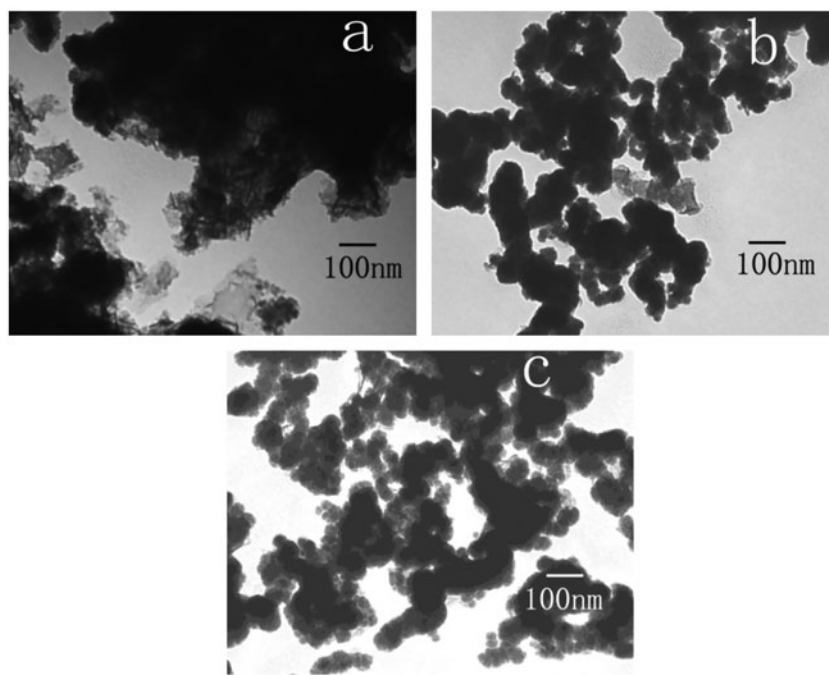
Fig. 3. TEM images of Pd/Fe NPs: (a) pristine Pd/Fe NPs, (b) PVP-Pd/Fe NPs (ethanol adding ratio is 0), (c) PVP/Ethanol-Pd/Fe NPs (ethanol adding ratio is 1:3).
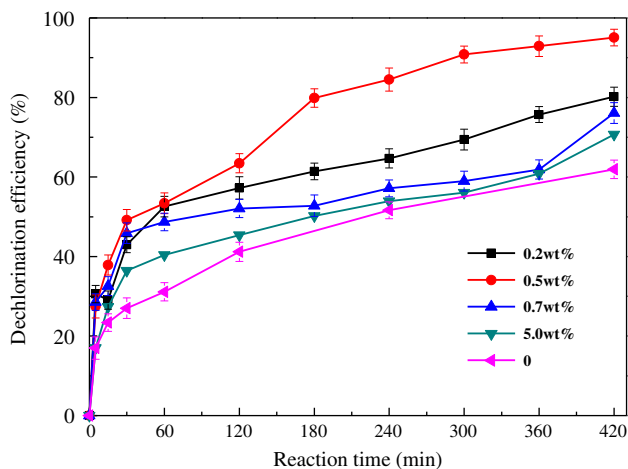
Fig. 4. Effect of PVP concentration on dechlorination efficiency of 2,4-DCP ($C_0 = 20$ mg/L, $\rho_{Pd/Fe} = 10$ g/L, initial pH = 7.0, $T = 25$℃).

Fig. 5, the dechlorination efficiency of 2,4-DCP by modified Pd/Fe NPs could be significantly increased with the addition ethanol. In this study, the optimal ethanol addition ratio is 1:5. From Fig. 5, when the ethanol addition ratio is less than 1:5, the dechlorination efficiency of 2,4-DCP increased with the increase of ethanol addition. When that ratio is larger than 1:5, the dechlorination rate decreased. The most likely explanation for the decrease of dechlorination efficiency at ethanol rate >1:5 might be due to the fact that the dissolution ratio of ferrous sulfate heptahydrate and potassium borohydride might be decreased with increasing ethanol addition ratio. And then synthetic product of ZVI NPs could be affected due to
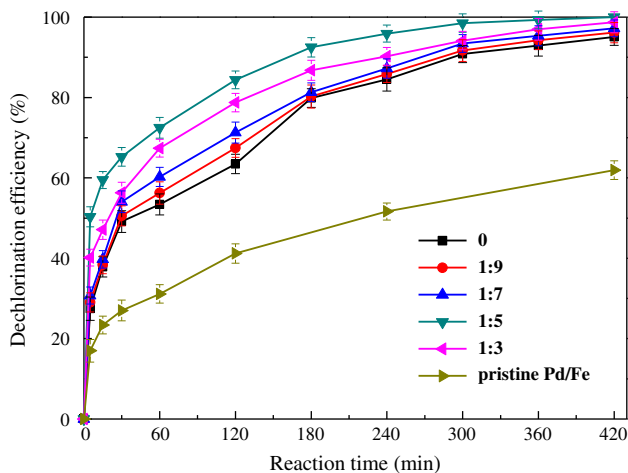
the free and strongly polarized hydroxyl groups of ethanol. These groups can form chelate bond between the metal irons in the aqueous solution, which was tightly wrapped around the metal ions that result in the formation of a limited shape of the finite structure. And this finite structure was in favor of the decrease of particle agglomeration and the increase of dispersing NPs. Therefore, when PVP and ethanol acted as a disperse system, PVP and ferrous sulfate heptahydrate aqueous solution mass ratio was 0.5 wt%, and the optimized addition ratio of ethanol in aqueous solution was 1:5.

3.3. Factors affecting the removal of 2,4-DCP

3.3.1. Dosage of Pd/Fe NPs

The removal efficiency of 2,4-DCP with reaction time from 0 min to 7 h under different addition dosage of pristine Pd/Fe, PVP-Pd/Fe, and PVP/ethanol-Pd/Fe NPs were calculated according to Eq. (4), and the results are shown in Fig. 6.

$$\text{Removal efficiency} = \frac{C_0 - C_t}{C_t} \times 100\% \qquad (4)$$

where C_0 and C_t represent the concentrations of 2,4-DCP at time 0 and t, respectively. Fig. 6(a) shows that 2,4-DCP removal efficiency was greatly affected by the dosage of Pd/Fe NPs. As the dosage of PVP-Pd/Fe increased from 4 to 10 g/L, the dechlorination rate increased from 57 to 87%. And about 45% of 2,4-DCP was removed within 60 min. It can be seen from Fig. 6(b) that removal efficiency of 2,4-DCP changed greatly with dechlorination reaction time. At relatively low dosage (4 g/L PVP-Pd/Fe NPs), approximately 93% of 2,4-DCP was removed after 7 h. The removal efficiency of 2,4-DCP increased with increasing PVP/ethanol-Pd/Fe NPs dosage. Removal efficiency increased to 100% when the dosage is 10 g/L. From Fig. 6, no decrease of 2,4-DCP concentration was observed in the control batch reactor containing 2 g/L PVP. This indicates that the adsorption or partition of 2,4-DCP to PVP was negligible. Fig. 6 shows that 4 g/L of PVP-Pd/Fe and PVP/ethanol-Pd/Fe NPs exhibited better removal efficiency than 10 g/L bare Pd/Fe NPs. Less removal of 2,4-DCP by the pristine Pd/Fe NPs could be a result of the aggregation of the particles which indicate that the interactions between the particles and the contaminant are minimal. Fig. 6 shows that 10 g/L is the optimal dosage to the dechlorination of 2,4-DCP by two kinds of modified Pd/Fe NPs. Compared with PVP-Pd/Fe NPs, higher removal

Fig. 5. Effect of ethanol addition ratio on dechlorination efficiency of 2,4-DCP ($C_0 = 20$ mg/L, $\rho_{Pd/Fe} = 10$ g/L, initial pH = 7.0, $T = 25$℃).
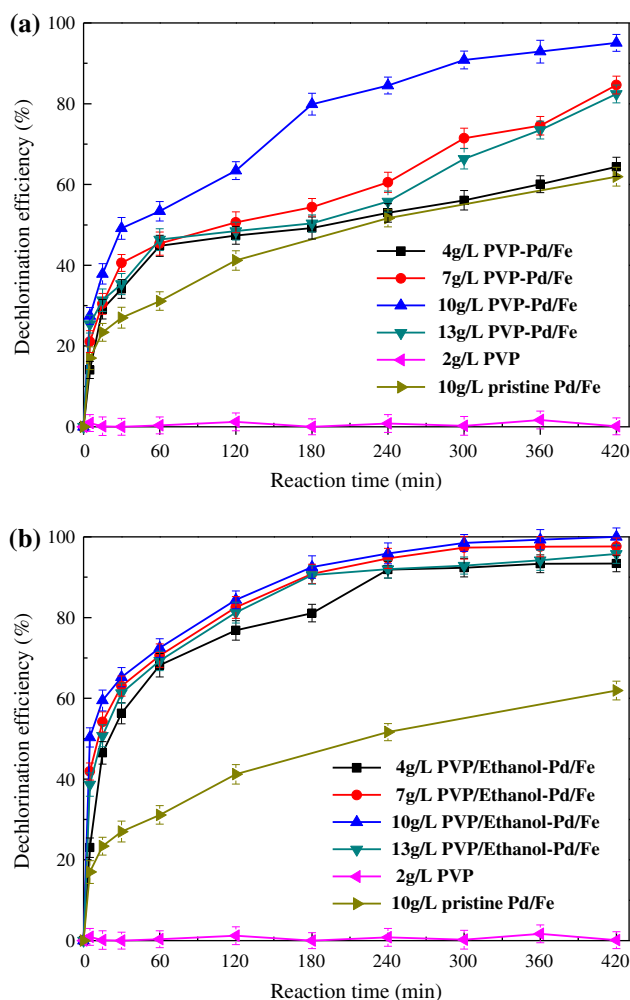
Fig. 6. Effect of particles amount on dechlorination activities of modified Pd/Fe NPs: (a) PVP-Pd/Fe NPs (PVP addition = 0.5 wt%, ethanol adding ratio is 0), (b) PVP-Pd/Fe NPs (PVP addition = 0.5 wt%, ethanol adding ratio is 1:5), $C_0 = 20$ mg/L, $T = 25$℃, initial pH = 7.0, Pd content = 0.1 wt%).

efficiency of PVP/ethanol-Pd/Fe NPs in Fig. 6(b) may be due to the adding of ethanol during the preparation of particles. Previous research have shown that the surface area concentration of the metal particles could be increased by increasing the amount of NPs dosage, and dechlorination efficiency of 2,4-DCP by Pd/Fe NPs could also be improved [29,30]. But only when Pd/Fe NPs dosage was within a certain range, dechlorination efficiency increased correspondingly. When the particles dosage outnumbered the optimal range, dechlorination efficiency has nothing to do with the particulate dosage. This phenomenon might be explained by the fact that excessive dosage of NPs could prevent Pd/Fe NPs from being fully mixed with the target contaminants. Thus, the dosage of Pd/Fe

NPs was optimized to 10 g/L in subsequent dechlorination experiments of 2,4-DCP.

3.3.2. Effect of pH value

The pH value is also an important factor for effective dechlorination of 2,4-DCP with dispersant-coated Pd/Fe NPs. To evaluate the effect of initial pH value of modified Pd/Fe NPs suspensions on dechlorination efficiency, as well as to optimize the pH condition, the desired pH values of the batch experiment solution were controlled by adding sodium hydroxide solution (0.1%) to increase pH value or sulfuric acid solution (0.1%) to decrease pH value ranging from 4 to 10.
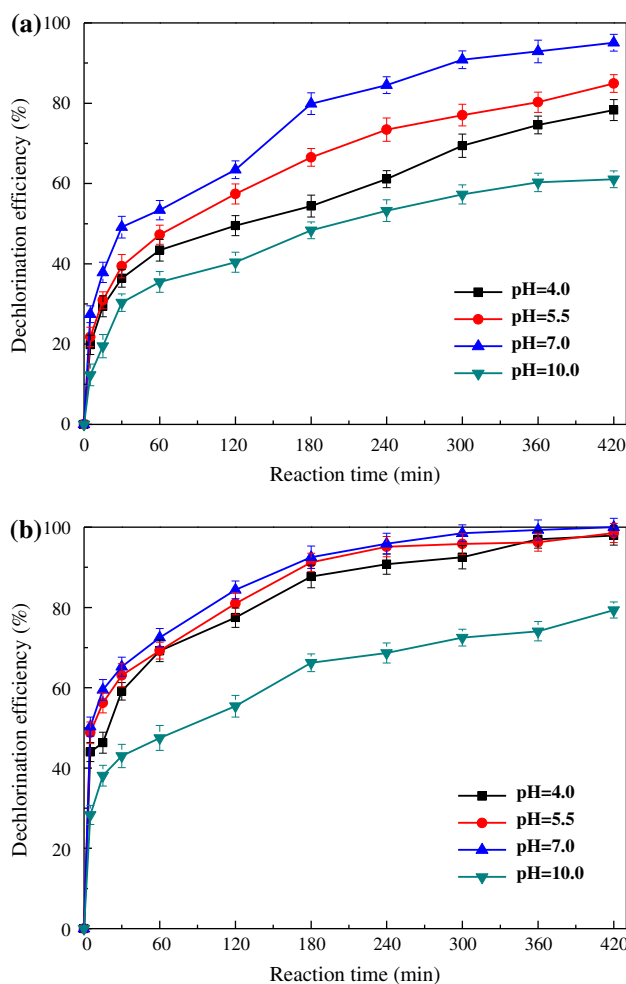
Fig. 7. Effect of initial pH value on dechlorination activities of dispersant-coated Pd/Fe NPs: (a) PVP-Pd/Fe NPs (PVP addition = 0.5 wt%, ethanol adding ratio is 0), (b) PVP-Pd/Fe NPs (PVP addition = 0.5 wt%, ethanol addition ratio is 1:5), $C_0 = 20$ mg/L, $\rho_{Pd/Fe} = 10$ g/L, $T = 25$℃, Pd content = 0.1 wt%).

From Fig. 7, higher dechlorination efficiencies were obtained at initial pH value of 7.0. In general, Pd/Fe NPs represented lower dechlorination activities under alkaline or acidic conditions, especially at pH value larger than 7.0 (such as pH = 10.0), dechlorination efficiencies were significantly reduced from the alkaline condition. Because the ferrous ions Fe^{2+} dissolved in reaction system might collided with hydroxyl ions, followed by the formation of ferrous hydroxide precipitation, resulting in occupation of reactive sites by the precipitates and decrease in dechlorination efficiency [27]. At pH lower than 7, excessive hydrogen gas bubbles produced by the erosion of ZVI NPs might largely prevent 2,4-DCP from approaching the modified Pd/Fe NPs, and hence resulting in the decrease of removal efficiency.

3.3.3. Effect of dechlorination temperature

The effect of temperature on the removal of 2,4-DCP was investigated. The solutions were incubated at different temperatures (25, 30, and 35℃) for 10 min before reactions. Fig. 8(a) shows that as the temperature increased from 20 to 35℃, the removal efficiency of 2,4-DCP increased from 87 to 95% within 7 h. Fig. 8 (b) showed that all the removal efficiencies of 2,4-DCP reached 50% in initial 5 min and 2,4-DCP was completely degraded in 7 h under three different temperature conditions. The results indicate that with the increase of reaction temperature, the dechlorination efficiency of 2,4-DCP by modified Pd/Fe NPs was increased. This phenomenon might be due to the following reason: with the increase of reaction temperature, the molecular collision frequency increased, and the percentage of the activated molecules of the reaction system was increased too, and resulted in the increase of dechlorination efficiency. And an important reason for the increase of dechlorination efficiency with the increase of reaction temperature is that 2,4-DCP dechlorination Pd/Fe NPs is a endothermic reaction.

3.4. Mechanism of dechlorination

In order to investigate the dechlorination mechanism of 2,4-DCP by PVP/Ethanol-modified Pd/Fe NPs, the intermediate and final products during dechlorination process were determined. As shown in Fig. 9, the intermediate products were 2-CP and 4-CP. P was the final product for catalytic dechlorination of 2,4-DCP by PVP/Ethanol-Pd/Fe NPs. 2,4-DCP was completely degraded in 300 min, and intermediate products, 2-CP and 4-CP, were produced. At 30 min
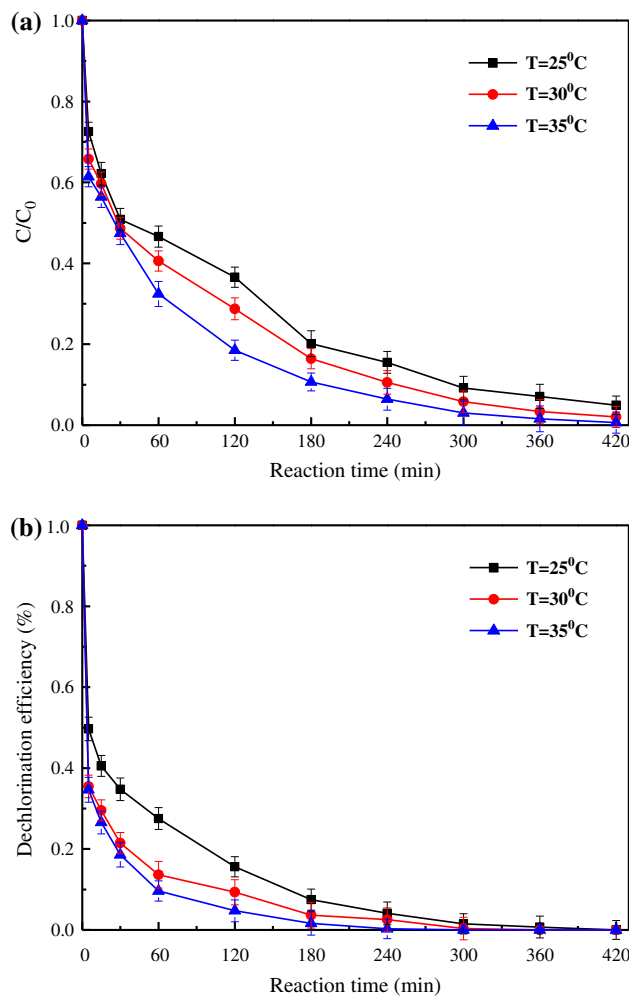
Fig. 8. Effect of temperature on dechlorination activities of modified Pd/Fe NPs: (a) PVP-Pd/Fe NPs (PVP addition = 0.5 wt%, ethanol adding ratio is 0), (b) PVP-Pd/Fe NPs (PVP addition = 0.5 wt%, ethanol adding ratio is 1:5), $C_0 = 20$ mg/L, $\rho_{Pd/Fe} = 10$ g/L, initial pH = 7.0, Pd content = 0.1 wt%).

of dechlorination reaction, the concentration of intermediate products increased to the maximum, and then gradually reduced. The amount of final product P had an increasing trend from 0 min to 420 min. Throughout the duration of the dechlorination reaction, most 2,4-DCP was converted into P, and only a small amount of 2-CP and 4-CP were generated, followed by the degradation of 2-CP and 4-CP into P. The reactants and products might not meet the mass balance from Fig. 9, that phenomenon might be explained by the absorption of some dechlorination products on PVP/Ethanol-Pd/Fe NPs.

Removal of 2,4-DCP by PVP/Ethanol-modified Pd/Fe NPs had a complicated reaction path, the over-
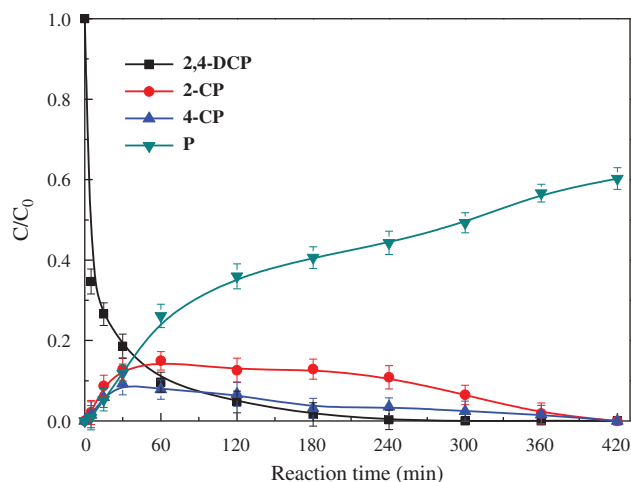
Fig. 9. Transformation of 2,4-DCP by PVP/Ethanol-Pd/Fe NPs (initial 2,4-DCP concentration (C_0) was 20 mg/L, Pd/Fe loading was 10 g/L, initial pH was 7.0, reaction temperature was 35°C).

Fig. 10. Dechlorination rate of 2,4-DCP by Pd/Fe NPs. Initial 2,4-DCP concentration (C_0) was 20 mg/L, Pd/Fe loading was 10 g/L, initial pH was 7.0, reaction temperature was 35°C.

all removal rate was described using the pseudo-first-order kinetic equation:

$$-\ln\left(\frac{C}{C_0}\right) = k_{obs} \cdot t \quad (5)$$

$$v = -\frac{dc}{dt} = k_{SA} a_S \rho_m = k_{obs} \cdot C \quad (6)$$

where C_0 is the initial 2,4-DCP concentrations (mg L^{-1}), C is the concentration (mg L^{-1}) of 2,4-DCP in solution, respectively; t is the reaction time (min) and the values of k_{obs} is the observed rate constant and calculated from the slope of the line for $\ln(C/C_0)$ vs. time; k_{SA} is the specific reaction rate constant based on surface areas of the three Pd/Fe NPs and modified Pd/Fe NPs; a_S is the specific surface area of Pd/Fe NPs; and ρ_m is the mass concentration of NPs. In this study, the surface areas of pristine Pd/Fe, PVP-Pd/Fe, and PVP/ethanol-Pd/Fe were 26.8, 23.3, and 25.4 m^2 g^{-1}, respectively. ρ_m is 10 mg L^{-1}. Fig. 10 is the comparison of 2,4-DCP dechlorination by using modified Pd/Fe NPs and pristine Pd/Fe NPs. And

the observed reaction rate constants k_{obs} and k_{SA} were calculated for Pd/Fe NPs which are shown in Table 1. As can be seen from Fig. 10 and Table 1, dechlorination rates of 2,4-DCP by the three kinds of particles follow the order of PVP/ethanol-Pd/Fe > PVP-Pd/Fe > pristine Pd/Fe. Fig. 11 is schematic diagram of PVP-modified Fe NPs. Because of the presence of a carbonyl group in PVP, the metal particles and PVP are bonded together through the urging force, therefore, NPs could be effectively dispersed.

Evaluating reaction rates under different temperatures is an effective way to investigate reaction mechanisms. A chemical reaction has larger temperature dependence than a physical process. In this study, the

Table 1
k_{obs}, k_{SA} and R^2 values for catalytic dechlorination of 2,4-DCP with unmodified and PVP modified Pd/Fe NPs

	k_{obs}	k_{SA}	R^2
Pristine-Pd/Fe	0.39×10^{-2}	1.45×10^{-5}	0.9877
PVP-Pd/Fe	1.06×10^{-2}	4.55×10^{-5}	0.9944
PVP/Ethanol-Pd/Fe	1.91×10^{-2}	7.52×10^{-5}	0.9784
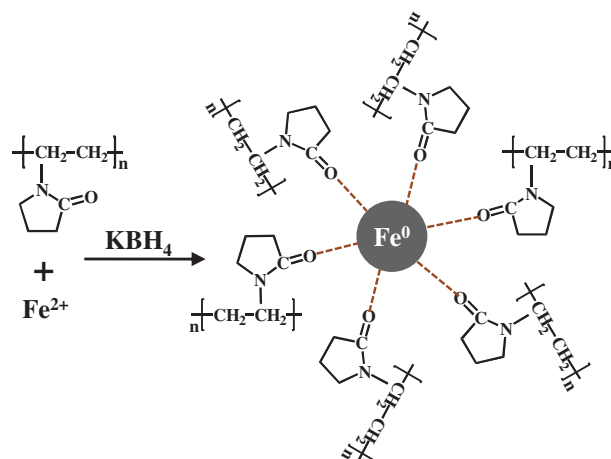
Fig. 11. A schematic of Fe nanoparticles stabilized with PVP.

(a)

(b)
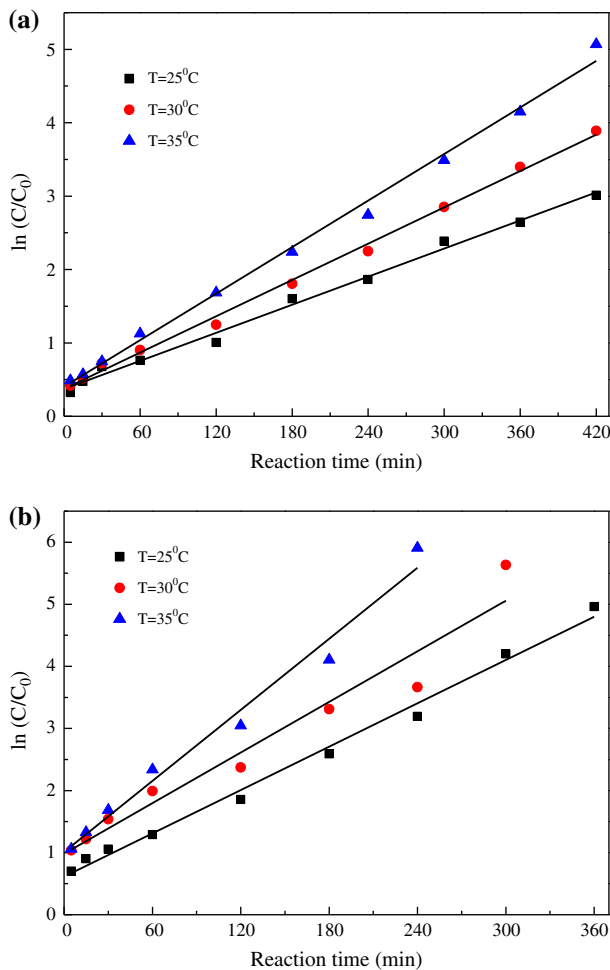
Fig. 12. Dechlorination of 2,4-DCP by modified Pd/Fe NPs at different temperatures. (a) PVP-Pd/Fe NPs, (b) PVP/ethanol-Pd/Fe NPs. ($C_0 = 20$ mg/L, $\rho_{Pd/Fe} = 10$ g/L, initial pH = 7.0, Pd content = 0.1 wt%).

surface, and the diffusion of a product back into solution. Previous studies have shown that diffusion-controlled reactions in solution have relatively low-activation energies (8–21 kJ/mol). On the contrary, the diffusion-controlled reactions in solution have relatively low-activation energies (>29 KJ/mol).

The correlations between the negative logarithm of C/C_0 and the reaction time during the catalytic dechlorination of 2,4-DCP-modified Pd/Fe NPs within 25–35°C are shown in Fig. 12. The observed reaction rate constants were obtained from the slope of the fitting line, and are summarized in Table 2.

An Arrhenius equation can be used to describe the relationship between the observed reaction rate constants and temperature was applied:

$$k_{obs} = Ae^{\frac{E_a}{RT}} \tag{7}$$

where A is a frequency factor, E_a is the activation energy, R is the ideal gas constant, and T is temperature. And Eq. (7) can be manipulated into Eq. (8):
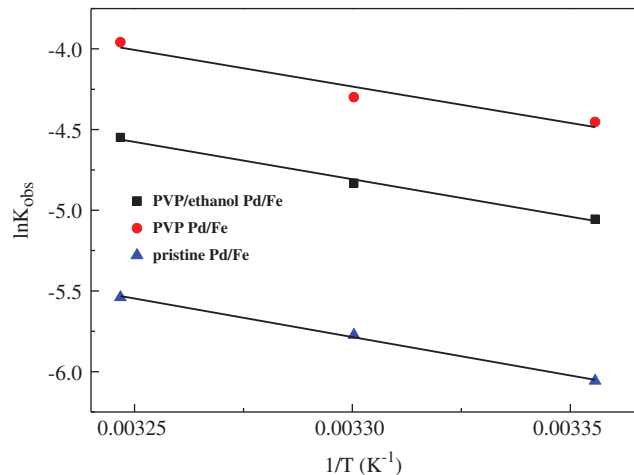
Fig. 13. Arrhenius plot for the estimation of activation energy: 2,4-DCP dechlorination by pristine Pd/Fe NPs and modified Pd/Fe NPs.

effect of temperature on the reaction rates of dechlorination 2,4-DCP by modified Pd/Fe was investigated. Generally, such a heterogeneous reaction as the dechlorination of 2,4-DCP by Pd/Fe NPs may involve several steps. These steps include the diffusion of a reactant to the surface, a chemical reaction on the

Table 2
k_{obs} and R^2 values for catalytic dechlorination of 2,4-DCP with dispersant-coated Pd/Fe NPs

Temperature (°C)	PVP-Pd/Fe		PVP/ethanol-Pd/Fe	
	k_{obs}	R^2	k_{obs}	R^2
25	0.64×10^{-2}	0.9923	1.16×10^{-2}	0.9915
30	0.83×10^{-2}	0.9964	1.36×10^{-2}	0.9444
35	1.06×10^{-2}	0.9944	1.91×10^{-2}	0.9784

Table 3
The k_{obs} values of different Pd/Fe NPs

Temperature (℃)	PVP Pd/Fe k_{obs}	PVP/ethanol Pd/Fe k_{obs}	PVDF-g-AA Pd/Fe k_{obs}	Free suspended Pd/Fe k_{obs}
25	0.64×10^{-2}	1.16×10^{-2}	1.22×10^{-2}	0.58×10^{-2}
30	0.83×10^{-2}	1.36×10^{-2}	–	–
35	1.06×10^{-2}	1.91×10^{-2}	1.7×10^{-2}	0.72×10^{-2}

$$\ln k_{obs} = -\frac{E_a}{RT} + \ln A \qquad (8)$$

Hence, a plot of the natural logarithm of k_{obs} vs. the reciprocal of temperature would result in a linear relationship with a slope equal to $-E_a/R$. Fig. 13 illustrates the Arrhenius plots of the natural logarithm of k_{obs} vs. $1/T$ for the 2,4-DCP dechlorination by modified Pd/Fe NPs. From the slopes of the plots the activation energies of 2,4-DCP dechlorination by pristine Pd/Fe, PVP-Pd/Fe, and PVP/ethanol-Pd/Fe-modified Pd/Fe NPs were 39.58, 38.50, and 37.63 kJ/mol, respectively. Obviously, the activation energies in three kinds of catalytic dechlorination systems were greater than 29 kJ/mol, which indicated that the surface chemical reaction was the rate-limiting step in the 2,4-DCP dechlorination process, and the dechlorination of 2,4-DCP is a endothermic reaction.

Xia et al. [31] modified poly (vinylidene fluoride) (PVDF) film to increase its hydrophilicity. Monochloroacetic acid was dechlorinated by using Pd/Fe NPs fixed in modified PVDF film. Table 3 shows the k_{obs} values of free suspended Pd/Fe and Pd-Fe/PVDF-g-AA dechlorination of monochloroacetic acid in literature and the k_{obs} values of PVP-Pd/Fe, PVP/ethanol-Pd/Fe dechlorination of 2,4-DCP in our manuscript. As can be seen from Table 3, the k_{obs} values of PVP, PVP/ethanol and PVDF-g-AA modified Pd/Fe NPs are bigger than free suspended Pd/Fe. This shows that, compared to pristine Pd/Fe NPs, modified Pd/Fe have a higher reactivity. By comparing the three kinds of modification methods, the k_{obs} values of PVP/ethanol and PVDF-g-AA-modified Pd/Fe are very close, and bigger than that of PVP-Pd/Fe. From Table 3, the conclusion of use PVP and PVP/ethanol-modified Pd/Fe NPs can achieve the desired results.

4. Conclusions

In this study, we used PVP and PVP/ethanol to modified Pd/Fe NPs. And the effects of PVP on the dispersity and dechlorination behaviors of modified Pd/Fe NPs were investigated; dechlorination conditions of PVP-modified Pd/Fe NPs were optimized. The obtained results are as follows:

(1) Pd/Fe NPs were modified with PVP and PVP/ethanol to under inert conditions, respectively. And the characterization results show the modified Pd/Fe NPs displayed greater dispersion than pristine Pd/Fe NPs.
(2) Compared to pristine Pd/Fe NPs, PVP, and PVP/Ethanol coated Pd/Fe NPs showed 25–38% higher dechlorination efficiency for removal of 2,4-DCP under optimized dispersant addition.
(3) Moderate pH or acidic conditions were more suitable for dechlorination of 2,4-DCP by pristine and modified Pd/Fe NPs at a temperature of 35℃. And the optimized dosage of Pd/Fe NPs was 10 g/L.
(4) Activation energies of pristine Pd/Fe, PVP-Pd/Fe, and PVP/ethanol-Pd/Fe NPs were calculated to be 39.47, 38.50, and 37.63 kJ/mol, respectively.

References

[1] USEPA, The inventory of sources of dioxin in the United States, EPA/600/P98/00A2, 1998.
[2] L.Q. Xing, J. Sun, H.L. Liu, Combined toxicity of three chlorophenols 2,4-dichlorophenol, 2,4,6-trichlorophenol and pentachlorophenol to daphnia magna, J. Environ. Monit. 14 (2012) 1677–1683.
[3] X.W. Jin, J.M. Zha, Y.P. Xu, Z.J. Wang, S.S. Kumaran, Derivation of aquatic predicted no-effect concentration (PNEC) for 2,4-dichlorophenol: Comparing native species data with non-native species data, Chemosphere 84 (2011) 1506–1511.
[4] R.W. Gillham, S.F. O'Hannesin, Development of zero-valent iron as an *in situ* reactant for remediation of VOC-contaminated groundwater. Groundwater remediation: Existing technology and future directions. Association of Groundwater Scientist and Engineers, 9–12 October 1994, Las Vegas, NV.

[5] R.W. Gillham, S.F. O'Hannesin, Enhanced degradation of halogenated aliphatics by zero-valent iron, Ground Water 32 (1994) 958–967.

[6] F. Fagerlund, T.H. Illangasekare, T. Phenrat, H.J. Kim, G.V. Lowry, PCE dissolution and simultaneous dechlorination by nanoscale zero-valent iron particles in a DNAPL source zone, J. Contam. Hydrol. 131 (2012) 9–28.

[7] X.H. Xu, H.Y. Zhou, D.H. Wang, Catalytic dechlorination of chlorobenzene in water by Pd/Fe system, Chin. Chem. Lett. 14 (2003) 700–703.

[8] V. Janda, P. Vasek, J. Bizova, Z. Belohlav, Kinetic models for volatile chlorinated hydrocarbons removal by zero-valent iron, Chemosphere 54 (2004) 917–925.

[9] Y. Han, W. Li, M.H. Zhang, Catalytic dechlorination of mono-chlorobenzene with a new type of nanoscale Ni(B)/Fe(B) bimetallic catalytic reductant, Chemosphere 72 (2008) 53–58.

[10] C.L. Chun, D.R. Baer, D.W. Matson, J.E. Amonette, R.L. Penn, Characterization and reactivity of iron nanoparticles prepared with added Cu, Pd, and Ni, Environ. Sci. Technol. 44 (2010) 5079–5085.

[11] T. Phenrat, N. Saleh, K. Sirk, R.D. Tilton, G.V. Lowry, Aggregation and sedimentation of aqueous nanoscale zerovalent iron dispersions, Environ. Sci. Technol. 41 (2007) 284–290.

[12] J. Su, S. Lin, Z.L. Chen, M. Megharaj, R. Naidu, Dechlorination of p-chlorophenol from aqueous solution using bentonite supported Fe/Pd nanoparticles: Synthesis, characterization and kinetics, Desalination 280 (2011) 167–173.

[13] N.S. Babu, N. Lingaiah, J.V. Kumar, P.S.S Prasad, Studies on alumina supported Pd-Fe bimetallic catalysts prepared by deposition-precipitation method for hydrodechlorination of chlorobenzene, Appl. Catal., A 367 (2009) 70–76.

[14] Z.H. Meng, H.L. Liu, Y. Liu, J. Zhang, S.L. Yu, F.Y. Cui, N.Q. Ren, J. Ma, Preparation and characterization of Pd/Fe bimetallic nanoparticles immobilized in PVDF·Al$_2$O$_3$ membrane for dechlorination of monochloroacetic acid, J. Membr. Sci. 372 (2011) 165–171.

[15] X.Y. Wang, C. Chen, H.L. Liu, J. Ma, Preparation and characterization of PAA/PVDF membrane-immobilized Pd/Fe nanoparticles for dechlorination of trichloroacetic acid, Water Res. 42 (2008) 4656–4664.

[16] E.H. Lee, M.k. Lee, C.K. Rhee, Preparation of stable dispersions of Ni nanoparticles using a polymeric dispersant in water, Mat. Sci. Eng.: A 449–451 (2007) 765–768.

[17] K. Peng, X.J. Yin, L.P. Zhou, J.J. Zhu, A.P. Hu, H. Jin, Y.W. Du, Influence of dispersant on the morphology of silica-coated cobalt nanoparticles synthesized by a wet based method, Mater. Chem. Phys. 119 (2010) 351–354.

[18] H.S. Wang, X.L. Qiao, J.G. Chen, X.J. Wang, S.Y. Ding, Mechanisms of PVP in the preparation of silver nanoparticles, Mater. Chem. Phys. 94 (2005) 449–453.

[19] B.W. Zhu, T.T. Lim, J. Feng, Influences of amphiphiles on dechlorination of a trichlorobenzene by nanoscale Pd/Fe: Adsorption, reaction kinetics, and interfacial interactions, Environ. Sci. Technol. 42 (2008) 4513–4519.

[20] F. He, D. Zhao, Manipulating the size and dispersibility of zerovalent iron nanoparticles by use of carboxymethyl cellulose stabilizers, Environ. Sci. Technol. 41 (2007) 6216–6622.

[21] F. He, D. Zhao, Preparation and characterization of a new class of starch-stabilized bimetallic nanoparticles for degradation of chlorinated hydrocarbons in water, Environ. Sci. Technol. 39 (2005) 3314–3320.

[22] F. He, D. Zhao, J. Liu, C.B. Roberts, Stabilization of Fe-Pd nanoparticles with sodium carboxymethyl cellulose for enhanced transport and dechlorination of trichloroethylene in soil and groundwater, Ind. Eng. Chem. Res. 46 (2007) 29–34.

[23] A. Tiraferri, K.L. Chen, R. Sethi, M. Elimelech, Reduced aggregation and sedimentation of zero-valent iron nanoparticles in the presence of guar gum, J. Colloid Interface Sci. 324 (2008) 71–79.

[24] F. He, D.Y. Zhao, Preparation and characterization of a new class of starch-stabilized bimetallic nanoparticles for degradation of chlorinated hydrocarbons in water, Environ. Sci. Technol. 39 (2005) 3314–3320.

[25] P.R. Chang, P.W. Zheng, B.X. Liu, D.P. Anderson, J.G. Yu, X.F. Ma, Characterization of magnetic soluble starch-functionalized carbon nanotubes and its application for the adsorption of the dyes, J. Hazard. Mater. 186 (2011) 2144–2150.

[26] A. Tiraferri, K.L. Chen, R. Sethi, M. Elimelech, Reduced aggregation and sedimentation of zero-valent iron nanoparticles in the presence of guar gum, J. Colloid Interface Sci. 324 (2008) 71–79.

[27] L. Guo, Q.J. Huang, X.Y. Li, S.H. Yang, PVP-coated iron nanocrystals: Anhydrous synthesis, characterization, and electrocatalysis for two species, Langmuir 22 (2006) 7867–7872.

[28] H. Chen, H.J. Luo, Y.C. Lan, T.T. Dong, B.J. Hu, Y.P. Wang, Removal of tetracycline from aqueous solutions using polyvinylpyrrolidone (PVP-K30) modified nanoscale zero valent iron, J. Hazard. Mater. 192 (2011) 44–53.

[29] J. Gotpagar, E. Grulke, T. Tsang, D. Bhattacharyya, Reductive dehalogenation of trichloroethylene using zero-valent iron, Environ. Prog. 16 (1997) 37–143.

[30] C. Chen, X.Y. Wang, Y. Chang, H.L. Liu, Dechlorination of disinfection by-product monochloroacetic acid in drinking water by nanoscale palladized iron bimetallic particle, J. Environ. Sci. 20 (2008) 945–951.

[31] Z. Xia, H.L. Liu, S. Wang, Z.H. Meng, N.Q. Ren, Preparation and dechlorination of a poly(vinylidene difluoride)-grafted acrylic acid film immobilized with Pd/Fe bimetallic nanoparticles for monochloroacetic acid, Chem. Eng. J. 200–202 (2012) 214–223.